Mon. Not. R. Astron. Soc. **000**, 1–?? (2002) Printed 16 October 2012 (MN LaTeX style file v2.2)

arXiv:1210.3883v1 [astro-ph.GA] 15 Oct 2012

# The consequence of jet interacting with a warped disc

S.F. Zou[1] and B.P. Gong[1]*
[1] *Department of Physics, Huazhong University of Science and Technology, Wuhan 430074, China*

Accepted, Received ;

**ABSTRACT**
The sprinkler pivots on a bearing on top of its threaded attachment nut. It is driven in a circular motion by a spring-loaded arm pushed back by the water stream which returns to "impact" the stream. The water stream can thus rotate around a fix axis. Analogously in our universe, the outflow or jet formed by the relativistic plasma corresponds to the water stream of a sprinkler; and the baryons in the tilted outer accretion disc or torus play the role of "impact arm". Then the jet aligning with the inner parts of a warped disc can directly "touch" the outer region of the disc. The resultant collision between such rapid leptons and slow baryons automatically accounts for the main features of broad-line region of active galactic nuclei. Moreover, it naturally provides a channel of dissipating the angular momentum of an accretion disc, which has long been a problem in theory of accretion disc.

**Key words:** accretion,accretion discs—(galaxies:)quasars: general—galaxies:individual (3C120,3C279,3C273,3C345,OJ287)

## 1 INTRODUCTION

An active galactic nucleus (AGN) is comprised of three major elements, an accretion disc, a central spinning black hole (BH), and a jet. The complex interactions among them result in fascinating phenomena of all bands, from radio, optical to X-ray and Gamma-ray, and displaying in all forms, from images to spectra and time varying effects. Although tremendous progresses have been made in understanding the mechanisms underlying them, many fundamental questions are still open.

Firstly, frame dragging produced by a rotating BH with angular momentum $S$ causes precession of a particle if its orbital plane is inclined in relation to the equatorial plane of the rotation object. This is known as the Lense-Thirring effect (Lense & Thirring 1918), with a precession velocity, $\Omega_{LT} \propto 1/r^3$, of strong function of radius, $r$, so that the inner parts of the disc tends to align with the direction of the BH spin.

In the case where the BH spin is misaligned with the rotation direction of the disc, the disc becomes twisted and warped. Such a warp can propagate in the disc in a diffusive manner through viscosity (Pringle 1992). And the warp can make a large increase in the accretion rate (Lodato & Pringle 2006).

On the other hand, when a BH is in a binary system, the inner regions of the disc remain aligned with the spin of the central BH. Whereas, the outer region precesses around the orbital axis, owing to the tidal torque of the companion object (Katz 1973; Sillanpää et al. 1988; Katz 1997; Romero et al. 2000; Caproni & Abraham 2004b; Martin et al. 2009b). This results in a warped and twisted disc.

The apparent lack of correlation between the orientation of the radio jets and the plane of the host galaxies disc might also be attributed to warped discs (Schmitt et al. 2002).

Then there is a question: what if a disc is so warped that the jet axis aligning with the inner disc touches the outer disc? Once such a warp induced jet-disc interaction occurs, the inner and outer parts of a warped disc interact in a new way other than the viscosity, which influences the precession velocity of jet, accretion rate and stability of the disc.

Secondly, accretion disc has been proven to be one effective mechanism of extracting gravitational potential energy and converting it to radiation powering AGNs. No matter a disc is warped or not, the accreted material at the inner region of the disc has to dissipate its angular momentum in order to fall on to the BH. If there is no external torque, the angular momentum loss is achieved through the accretion disc by outwardly transferring angular momentum. Accretion onto an AGN black hole will be limited largely by how rapidly angular momentum can be lost, which determines the power of AGN directly. The angular momentum transferred to the periphery must have a reasonable way of loss,

---

* E-mail: bpgong@mail.hust.edu.cn

© 2002 RAS

or the accumulation of external angular momentum would cause instability in the accretion disc.

Thirdly, one of the fundamental and defining characteristics of AGNs is the presence of broad emission lines in their optical and ultraviolet (UV) spectra. The investigation of the profile and intensities of these lines show that they originate in dense gas moving very fast around the central engine, which are thought to be fully exposed to the intense radiation from the engine.

The outer region of disc and wind from disc as possible origins of BLR have been studied extensively (Eracleous et al. 2009). However, the complexity of observations, e.g., the double-peaked broad emission lines are thought to originate in disc, while the local viscosity heating is usually insufficient for the observed luminosity of the emission site; and the correlation of BLR (optical and UV) with Fe K$\alpha$ (X-ray) lines indicate that the origin of BLR is still an open question.

Interestingly, each of the three questions, the precession property, transfer of angular momentum, and origin of BLR, appears to be unrelated and difficult, but all of them together point to a simple scenario: sprinkler, with the water stream replaced by the jet and "impact arm" replaced by the outer parts of accretion disc.

The collision between jet (formed by relativistic electrons) and the outer disc (slow baryons), automatically kicked out baryons from the disc, which provides a channel of angular momentum dissipation of a disc. Moreover, such a jet disc interaction influences the overall precession velocity of the disc. Finally, the baryons in the disc, carrying velocity gained through the collision with electrons, spread around the collision site, which naturally account for the major features of BLR.

Therefore, sprinklers in our yards, may provide a clue to understand what happens to "sprinklers" of the garden of universe.

## 2 THE NEW MODEL

Once a disc is warped as shown in Fig.1, the jet-disc interaction occurs. The collision sites separate from the central engine by a distance $r_0$. The opening angle of the jet cone is denoted, $\theta_0$, and the misalignment angle between the jet axis and the axis of the precession cone is $\alpha_0$, as shown in Fig.1.

## 3 TRANSFER OF ANGULAR MOMENTUM

At different radii of a disc, gaseous material is orbiting with differing angular velocities, $\Omega$, determined by Kepler's third law. Because of the ever present chaotic thermal motions of fluid molecules or turbulent motions of fluid elements, viscous stresses are generated. This type of transport process is known as shear viscosity.

The torque exerted by the outer ring on the inner one (= −the torque of the inner on the outer) is $G(R) = 2\pi R\nu\Sigma\, R^2\, \frac{d\Omega(R)}{dR}$, where $\nu$ is the kinematic viscosity, $\Sigma$ is the surface density of the disc, and $\Omega(R)$ is the angular velocity. Such a torque corresponds to a transfer of angular momentum (per unit time) to the outermost ring,

$$\dot{L} \sim -G(r_0) = -2\pi\nu\Sigma\, R^3\, \frac{d\Omega}{dR}\,|_{R=r_0}\,. \tag{1}$$

The accretion rate of mass $\dot{M}$ can be expressed by,

$$\nu\Sigma = \frac{\dot{M}}{3\pi}[1-(\frac{R_*}{R})^{1/2}], \tag{2}$$

where $R_* = 2G\,M_p\,/\,c^2$ is the Schwarzschild radius of a BH.

Substitute the Kepler angular velocity, $\Omega = \Omega_K(R) = (GM_p/R^3)^{1/2}$, and Eq.2 into Eq.1, the angular momentum loss rate can be written in terms of $\dot{M}$,

$$\begin{aligned} \dot{L} &\sim \{-2\pi\, R^3 \cdot \tfrac{\dot{M}}{3\pi}[1-(\tfrac{R_*}{R})^{1/2}] \cdot \tfrac{-3}{2}(\tfrac{G\,M_p}{R^5})^{1/2}\}|_{R=r_0} \\ &= (G\,M_p)^{1/2}\,\dot{M}(r_0^{1/2} - R_*^{1/2}) \end{aligned}\quad. \tag{3}$$

Such a $\dot{L}$ is the angular momentum required to be transferred to outer disc per unit time in order to maintain persistence power of an AGN fueled by $\dot{M}$. There must be an efficient channel of angular momentum dissipation, otherwise the piled up angular momentum in the outer disc can cause instability of the disc and stops the accretion process.

The sprinkler scenario provides a simple answer. The collision between jet and disc results in scattering matters off the disc, which should be in Kepler motion around BH and hence carrying angular momentum. Such a mass loss rate of the outer disc can be estimated by, $\dot{m}_{loss} = M_{disc}\dot{L}/L_{disc}$, where $M_{disc} = nm_p$ and $L_{disc} = nL_p$ are mass and angular momentum of the disc respectively ($n$ is the total number of baryons in the disc).

If we use the angular momentum of the outermost ring to represent that of the whole disc, the mass loss rate reduces to

$$\dot{m}_{loss} \sim \frac{m_p\dot{L}}{L_p} = \dot{M}[1-(\frac{R_*}{r_0})^{1/2}]. \tag{4}$$

where $L_p = m_p\, r_0^2\, \omega_0 = m_p(G\,M_p\,r_0\,)^{1/2}$ is the angular momentum of a proton. Thus, a channel of dissipating angular momentum is set up, at a warped disc as shown in Fig.1.

## 4 THE COLLISION PROCESS

The jet-disc interaction dissipating the angular momentum can be calculated simply by the collision of relativistic leptons in the jet with the slow baryons in the outer disc, as shown in Fig.2. Major parameters in the study of such a jet-disc collision are: the volume of the interaction zone, $V_i$; the number density of baryons (dominantly protons) in the outermost disc, $n_p$; the number density of leptons (relativistic electrons) in the jet, $n_e$, which travel at speed, $v_e$. The number of leptons scattered into a solid angle between $\Theta$ and $\Theta + d\Theta$ per unit time is given,

$$d\,N_i = 2\pi\sigma(\Theta)\sin\Theta d\Theta \cdot n_e\,v_e \cdot n_p\,V_i\,. \tag{5}$$

The number of leptons ejected out from the jet per unit time is estimated, $N_e \sim \xi\dot{M}/\,m_p$, where $\xi$ is a dimensionless coefficient, $\xi = 1$ means accreted matter is totally ejected out. With an opening angle of jet, $\theta_0$, as shown in Fig.1, we have $n_e v_e = N_e/[\pi(\frac{1}{2}r_0\theta_0)^2]$. The change of linear momentum (per unit time) of leptons involving in collision is given, $d\,p_e = 2\sqrt{2\,m_e\,E}\sin\frac{\Theta}{2}d\,N_i$, where $E = \gamma_e\,m_e\,c^2$ is the energy of a relativistic electron, with mass $m_e$ and Lorentz factor $\gamma_e$. For simplicity, the Rutherford scattering cross section

(Goldstein et al. 2005), $\sigma(\Theta) = \frac{1}{4}(\frac{ZZ'\, e^2}{2E})^2 \csc^4\frac{\Theta}{2}$, is used, where $E$ is the energy of the scattering particle. Although it is derived in the case of a repulsive scattering process, it is still a good approximation in the collision of the jet and disc.

Since the collision occurs predominantly between electrons and protons, the interacting charges satisfy, $(ZZ')^2 = 1$. Substituting Eq.5 into the linear momentum change yields,

$$d\,p_e = \sqrt{2\,m_e\,E}(\frac{e^2}{2E})^2\,\frac{8\xi\dot{M}\,n_p\,V_i}{m_p\,r_0^2\,\theta_0^2}\,\frac{\cos\frac{\Theta}{2}}{\sin^2\frac{\Theta}{2}}d\Theta, \tag{6}$$

The mean force corresponding to the interaction is

$$F = \int_{\Theta_0}^{\pi} d\,p_e. \tag{7}$$

The number density of protons in the outermost ring is $n_p$, each proton occupies a volume $1/\,n_p$, the functional relationship between the impact parameter and the scattering angle is (Goldstein et al. 2005), $s = ZZ'e^2\cot\frac{\Theta}{2}/(2E)$. In such case, we have $s \leqslant n_p^{-1/3}$, the lower limit of the integral can be obtained by,

$$n_p^{-1/3} = \frac{ZZ'\,e^2}{2E}\cot\frac{\Theta_0}{2}. \tag{8}$$

Integrating Eq.7, we get

$$F = [\sqrt{1 + (\frac{2E}{e^2\,n_p^{1/3}})^2} - 1]\sqrt{2\,m_e\,E}(\frac{e^2}{2E})^2\,\frac{16\xi\dot{M}\,n_p\,V_i}{m_p\,r_0^2\,\theta_0^2}, \tag{9}$$

Eq.9 corresponds to a torque, $N = F\,r_0$, which makes the jet to precess around the core at angular velocity, $\vec{\Omega}_p$, determined by, $\vec{N} = \vec{\Omega}_p \times \vec{S}$, so that,

$$N = \Omega_p S \sin\alpha_0 = \frac{2\pi(1+z)S\sin\alpha_0}{P}, \tag{10}$$

where $P$ is the precession period measured in the observer's reference frame, and $S = GM_p^2|a_*|/c$ is the spin angular momentum of the primary BH, with $a_*$ its dimensionless angular momentum. Such a precession resembles a sprinkler, with water stream and impact arm replaced by the jet and the baryons at the outer disc respectively.

Thus, according to the collision process described by Eq.5 to Eq.10, the mass loss rate, $\dot{M}$, required to precess the jet at the period, $P$, is,

$$\dot{M} = \frac{\pi(1+z)m_p r_0\theta_0^2 G M_p^2|a_*|\sin\alpha_0}{8cn_pV_iP\sqrt{2m_eE}\rho^2[\sqrt{1+(\rho n_p^{1/3})^{-2}} - 1]}, \tag{11}$$

where $\rho = e^2/(2E)$. Fore simplicity, $\xi = 1$ is assumed in the calculation of Eq.11. Notice that $\dot{M}$ of Eq.11 represents mass loss rate of the relativistic jet, which is thought to be comparable to the accretion rate of Eq.3 derived from the angular momentum transfer of a disc.

The parameter spaces of $\dot{M}$, $r_0$ and $V_i$ corresponding to the two mechanisms given by Eq.3 and Eq.11, can be displayed through the observational parameters of the Seyfert 1 galaxy 3C 120 and the quasar 3C 345, as shown in Table 1.

Assuming $\theta_0 = 5^\circ$, $\alpha_0 = 60^\circ$, $\gamma_e = 10$, $\dot{M}_0 = 1\,M_\odot/yr$, $n_p \sim 10^{30}\,m^{-3}$, $|\,a_*\,| = 0.9$, the cross area can be obtained as shown in Fig.3. Notice that in Fig.3 the inclined lines correspond to Eq.11; and the solid vertical ones correspond to Eq.3 in which $\dot{L}$ is estimated under the binary model, with radius $r_0$ equivalent to the outer disc radius $r_d$ under the tidal torque (Papaloizou & Terquem 1995; Larwood 1997).

The shadowed area of Fig.3 corresponds to an acceptable parameters of collision process, the predicted torque of which can precess the jet at a period of tens of years, which is expected by Newtonian torque (Rieger 2004).

The volume of the collision region is estimated, $V_i \sim 2r_0\theta_0 \cdot \pi R_{ring}^2$, the magnitude of which can be inferred from the cross of vertical lines (correspond to different scenarios) with the inclined lines of Fig.3.

The shadowed area corresponds to the case that the 10yr precession period is driven by the Newtonian torque, so that the size of the outermost ring of the disc can be estimated, $R_{ring} \sim [V_i/(2\pi r_0\theta_0)]^{1/2}$, which is $\sim 3.5 \times 10^{11} m$ for 3C 120, and $\sim 7.4 \times 10^{13} m$ for 3C 345.

In contrast, if the ∼10yr precession period originates in the Lense-Thirring precession in a single BH, the jet-disc collision results in a twisted outer ring of the disc. Because the collision makes the liner momentum of baryons in the outer disc vary as Fig.2. Such a twisting of outer ring apparently changes with the jet precession, so that the whole disc, inner and outer, varies at the precession rate dominated by the inner disc.

## 5 BLR ORIGINATED IN COLLISION

As a result of the jet-disc collision, baryons in the outer disc scattered by high-speed leptons in jet spread around the collision site.

The momentum and energy exchange between slow baryons and relativistic electrons are shown in Fig.2. The velocity distribution of scattered baryons can be calculated simply by the conservation of momentum,

$$v = 2\sqrt{2\,\gamma_e}\frac{m_e}{m_p}c\cos\theta, \tag{12}$$

where $\gamma_e$ is the Lorenz factor of relativistic electrons, and $\theta = (\pi - \Theta)/2$, as shown in Fig.2, is the misalignment angle between the velocity of protons and the jet axis.

By Eq.12, the velocity gained by a baryon at one collision, is $\sim 10^3$km/s, which is responsible for the velocity inferred from the Doppler broadening of emission lines observed in AGNs.

Moreover, the jet-disc collision predicts a velocity distribution as shown in Fig.4, in which magnitude of velocity decreases with the increase of $\theta$. Such a velocity distribution of baryons predicts a bi-polar configuration of line emission.

In fact, Eq.12 is obtained ignoring the energy absorption by baryons, which can ionize the baryons. For simplicity, we can assume that a half of energy before collision is absorbed by the baryons, the magnitude of the baryon velocity $v$ of Eq.12, will be smaller. While in order of magnitude the conclusion drawn is unaffected.

Notice that the bi-polar corresponds to half opening angle of $(\pi - \Theta_0)/2$, and the smallest deflection angle $\Theta_0$ is given by Eq.8.

In fact, Eq.12 predicts a correlation: the velocity of baryons inferred from line broadening of BLR is inversely related to precession period of the jet.

This is easy to understand. The more the linear momentum exchange between electrons of jet and the baryons of the disc, the more the momentum and energy gain for the baryons, so that they travel faster. On the other hand, this corresponds to larger action and reaction forces between jet and disc, and hence larger torque on the jet, so that the jet precesses more rapidly (and shorter precession period). The rate of jet precession can be approximated, $\Theta \sim 2\pi/P$, which is so small that $v$ of Eq.12 can be written, $v \approx \sqrt{2\gamma_e}\frac{m_e}{m_p}c\Theta \propto \gamma_e^{1/2}/P$. The predicted correlation is supported by some AGNs with corresponding observations, as shown in Table 2.

## 6 DISCUSSION

Besides interpreting the difficulties in angular momentum transfer and precession velocity of jet, a number of observations concerning BLR likely favor the new model.

Firstly, the profiles of the broad lines observed at a high spectral resolution and signal-to-noise ratio, appear to be very smooth (Eracleous et al. 2009). The velocity distribution predicted by our model originates in the jet-disc collision, as shown in Fig.4, is automatically smooth.

Secondly, as shown in Fig.1, the new model actually implies a limited jet-disc interaction, in which only a small fraction of leptons in the jet is involved in the collision. Once the jet plunges into the outer ring heavily, or touches part of inner rings, the collimated jet can be destroyed. This may explain the observations of radio quiet quasars, with the largest emission line width among AGNs, but weak in radio emission.

Obviously, when a torus is outside the bi-polar configuration of BLR of an AGN , then obscurity of the BLR becomes more complicated. Therefore, a LOS with a relatively small misalignment angle with the jet axis tends to observe single peaked emission line of BLR, as some Seyfert type 1.

And if the misalignment between LOS and jet axis is relatively large, the obscurity depends on the angle of LOS with the normal direction of the outer ring. As shown in Fig.1, a large misalignment is favorable to observe double-peaked BLR, and a small one tends to be obscured, as Seyfert type 2 (which is absence of BLR emission).

Thirdly, a number of authors (Chen & Halpern 1989; Eracleous & Halpern 1994; Strateva et al. 2006, 2008) have pointed out that local viscous dissipation in the line-emitting region of accretion disc does not provide enough power to account for the observed emission line luminosity.

Apparently in our model this difficulty is naturally avoided. During the collision, as shown in Fig.1, baryons at the collision sites (or near) gain energy and momentum (linear), which can automatically ionize neutral hydrogen or other atoms. Typically, a non-relativistic proton can absorb $\sim$ 1eV in a head on collision with an electron of Lorentz factor 10 in the jet, which can well account for the energy required for line emission of BLR. And multi-collision processes can easily excite a hydrogen to UV band.

Moreover, if the jet contains certain fraction of baryons with a bulk Lorentz factor of 10 also, their collisions with the baryons in the outer disc correspond to an energy exchange of $\sim$ 1KeV, which is responsible for the energy required to invoke the line emission of Fe K$\alpha$.

Because NGC 7213 displays very close speeds inferred from its BLR and Fe K$\alpha$ lines, it is used as an evidence of BLR origin for Fe K$\alpha$ line (Bianchi et al. 2008).

From the point of view of the jet-disc interaction, the cross section of the relativistic electrons in the jet with the non-relativistic Hydrogen in the disc differs from that of relativistic protons in jet and non-relativistic iron in the disc.

Therefore, even if a source shows considerably discrepancy between speeds inferred from BLR and Fe K$\alpha$ lines, the emission lines may still be originated at the same site of collision. So evidence of common origin should be found in luminosity, number density, absorbtion extracted from the two types of emission lines.

Consequently, all these issues are realized at the expense of a warped disc, which makes the jet-disc interaction possible.

## REFERENCES

Bianchi, S. et al., 2008, MNRAS, 389, L52

Caproni, A., & Abraham, Z. 2004a, ApJ, 602, 625

Caproni, A., & Abraham, Z. 2004c, in IAU Symp. 222, The Interplay among Black Holes, Stars and ISM in Galactic Nuclei, ed. T. Storchi-Bergmann, L. C. Ho, & H. R. Schmitt (Cambridge: Cambridge Univ. Press), 83

Caproni, A., Mosquera Cuesta, H. J., & Abraham, Z. 2004, ApJ, 616, L99

Caproni, A., & Abraham, Z. 2004b, MNRAS, 349, 1218

Chen, K., & Halpern, J. P. 1989, ApJ, 344, 115

Decarli, R., Dotti, M., & Treves, A. 2011, MNRAS, 413, 39

Eracleous, M., & Halpern, J. P. 1994, ApJS, 90, 1

Eracleous, M., Lewis, K. T., & Flohic, H. M. L. G. 2009, NewAstRev, 53, 133

Goldstein, H., Poole, C., & Safko, J. 2005, Copy-editing: Classical Mechanics, 3rd edn. Higher Education Press, Beijing

Katz, J. I. 1973, Nature Phys. Sci., 276, 87

Katz, J. I. 1997, ApJ, 478, 527

Larwood J. D. 1997, MNRAS, 290, 490

Lense, J., & Thirring, H. 1918, Phys. Z., 19, 156

Lodato, G., & Pringle, J. E. 2006, MNRAS, 368, 1196L

Martin, R. G., Pringle, J. E., & Tout, C. A. 2009b, MNRAS, 400, 383

Papaloizou, J. C. B., & Terquem, C. 1995, MNRAS, 274, 987

Pringle, J. E. 1992, MNRAS, 258, 811P

Rieger, F. M. 2004, ApJ, 615, L5

Rokaki, E., Lawrence, A., Economou, F., & Mastichiadis, A. 2003, MNRAS, 340, 1298

Romero, G. E., Chajet, L., Abraham, Z., & Fan, J. H., 2000, A&A, 360, 57

Schmitt, H. R., Pringle, J. E., Clarke, C. J., & Kinney, A. L. 2002, ApJ, 575, 150

Sillanpää, A. et al., 1988, ApJ, 325, 628

Strateva, I. V. et al., 2006, ApJ, 651, 749

Strateva, I. V., Brandt, W. N., Eracleous, M., & Garmire, G. 2008, ApJ, 687, 869

Wang, T. G., & Zhang, X. G. 2003, MNRAS, 340, 793

## 7 ACKNOWLEDGMENTS

We thank Y.C. Zou, Q.W. Wu, and D.X Wang for useful discussion and comment. We also thank J.Y. Gong for his help in Figure. This research is supported by the National Natural Science Foundation of China, under grand NSFC11178011.

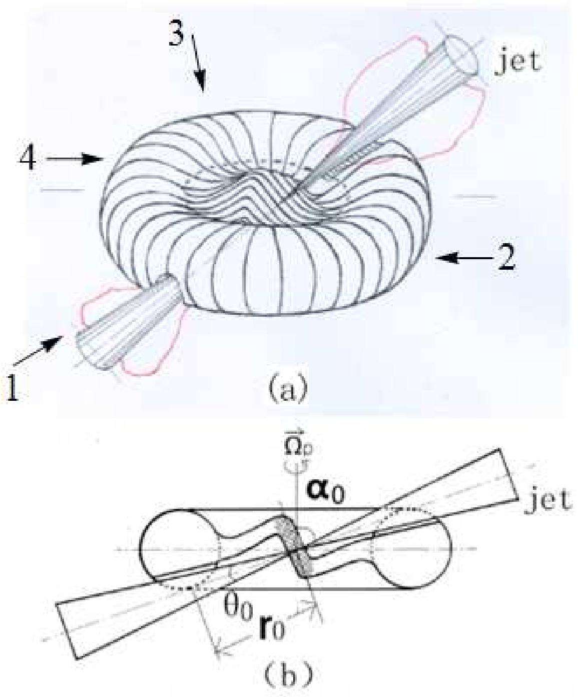

**Figure 1.** The interaction of a jet with a warped disc. At the collision site, baryons in the outermost ring of the warped disc are scattered off, which carry velocity of $\sim 10^3 km/s$, and are responsible for line emission, as represented by the cloudy configurations. In the figure, $r_0$ is the radius of the outermost ring, $\theta_0$ denotes the opening angle of the jet, $\alpha_0$ is the angle of the jet with the axis of the precession cone, and $\Omega_p$ is the precession angular velocity. Observing at different view angles, the BLR line profiles appear different, e.g., 1 is likely responsible for the single-peaked one; 3 for double-peak; and 2, 4 for absence of BLR lines (obscured by the warped disc or an outer torus co-plane with the outer disc).

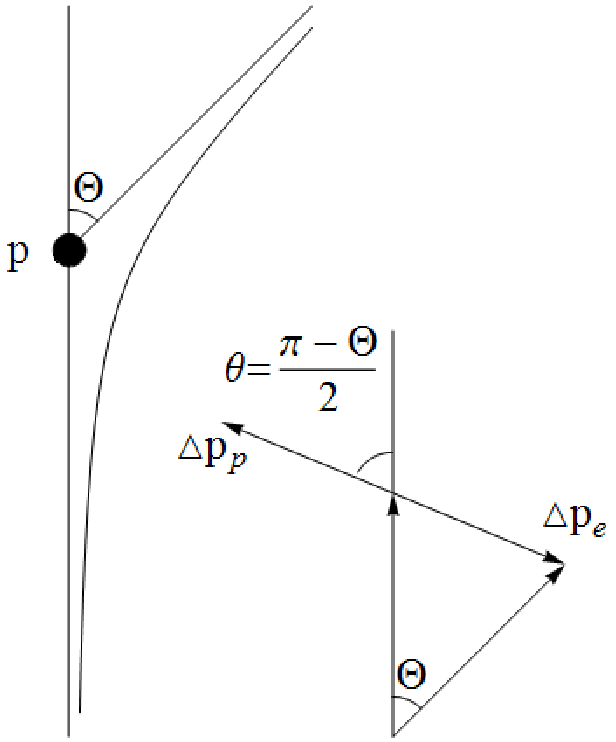

**Figure 2.** The schematic of collision of a relativistic lepton with a non-relativistic baryon. After colliding with a baryon at $p$. The trajectory of the lepton changes for an angle, Θ. The exchange of momenta between the lepton and the baryon is shown.

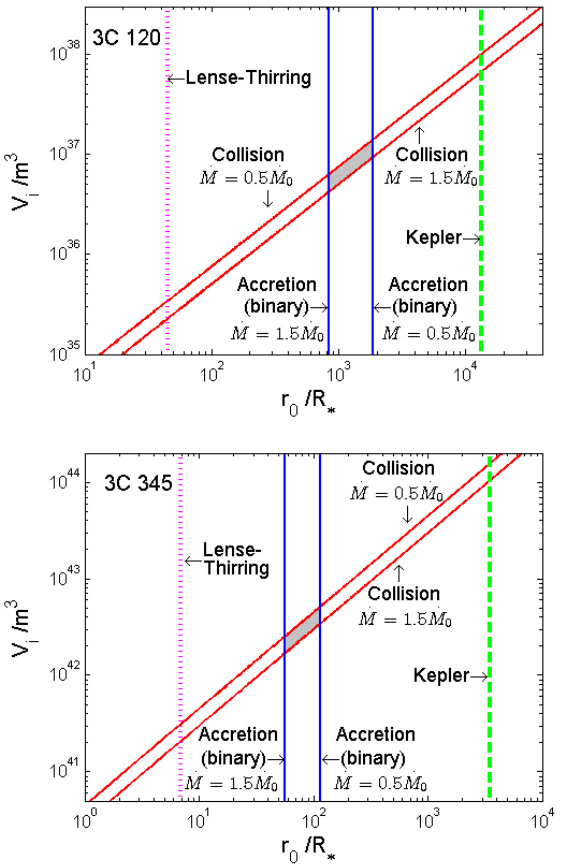

**Figure 3.** Parameters space of $V_i$ and $r_0$ predicted by the collision model for sources 3C 120 and 3C 345 respectively. The inclined lines correspond to the $V_i$ and $r_0$ relation given by Eq.11 with two different values of $\dot{M}$. The vertical ones in the middle (solid) correspond to $r_0$ given by Eq.3 under two different values of $\dot{M}$, which correspond to a collision site given by the tidal torque. The vertical line at right (dashed) is responsible for the radius where the Kepler velocity of gases is equal to that inferred from BLR emission lines. The vertical line at left (doted) corresponds to the disc radius when the Lense-Thirring precession yields a precession period of tens of years.

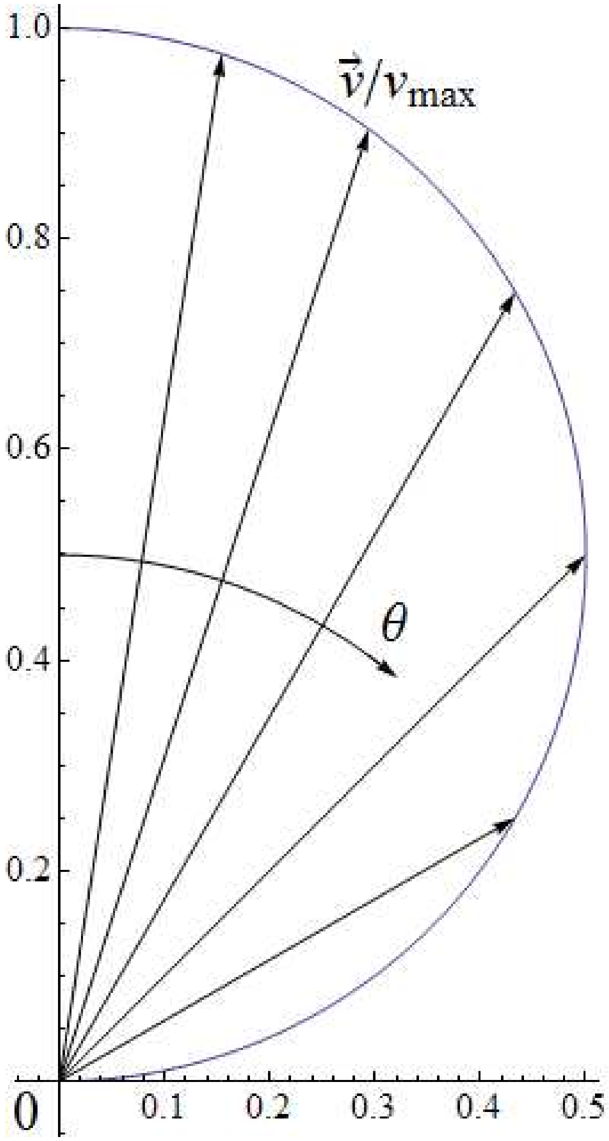

**Figure 4.** The velocity distribution of scattered baryons. The angle between the velocity of baryons and the jet axis is $\theta$, the magnitude of the velocity is given by $v = v_{\max}\cos\theta$, where $v_{\max} = 2\sqrt{2\gamma_e}m_e c/m_p$. Note that the velocity field is axial symmetric about the vertical axis, which predicts a bi-polar configuration of BLR speed.

**Table 1. Parameters of the Seyfert 1 galaxy 3C 120 and the quasar 3C 345 in the test of jet-disc collision**

| Object | $P(yr)$ | $M_p(M_\odot)$ | $M_s(M_\odot)$ | $P_{ps}(yr)$ | $r_{ps}(pc)$ | $z$ | $\varphi$ |
|---|---|---|---|---|---|---|---|
| 3C 120 | $^{a}12.3$ | $^{c}3.0\times10^{7}$ | $^{c}4.0\times10^{6}$ | $^{c}1.4$ | $^{c}0.002$ | 0.003 | $^{a}1.5^\circ\pm0.3^\circ$ |
| 3C 345 | $^{b}10.1$ | $^{c}4.4\times10^{9}$ | $^{c}3.6\times10^{9}$ | $^{c}5.2$ | $^{c}0.021$ | 0.5928 | $^{b}1.3^\circ\pm0.5^\circ$ |

NOTE.–$P$ is the precession period measured in the observer's frame, and $P_{ps}$ is the orbital period of the binary BH system. The mass of the primary and secondary BH are $M_p$ and $M_s$ respectively, $r_{ps}$ is the separation between the two BHs, $z$ is the redshift, and $\varphi$ is the half-opening angle of the precession cone given by the model of the following references.
REFERENCES.–a. Caproni & Abraham 2004b; b. Caproni & Abraham 2004a; c. Caproni & Abraham 2004c.

**Table 2. The correlation of precession period versus the FWHM of H$\alpha$ emission lines**

| Object | $z$ | $P(yr)$ | $P_{prec}(yr)$ | $FWHM\ (km\cdot s^{-1})$ |
|---|---|---|---|---|
| Arp 102B | 0.024 | $^{a}2.2$ | 2.148 | $^{b}14400$ |
| NGC 1097 | 0.004 | $^{a}5.5$ | 5.478 | $^{b}7200$ |
| 3C 345 | 0.593 | $^{a}10.1$ | 6.340 | $^{c}3600$ |
| OJ 287 | 0.306 | $^{a}11.6$ | 8.882 | $^{d}3710$ |
| 3C 120 | 0.033 | $^{a}12.3$ | 11.907 | $^{c}1846$ |
| 3C 273 | 0.158 | $^{a}16.0$ | 13.817 | $^{c}3260$ |
| 3C 279 | 0.536 | $^{a}22.0$ | 14.323 | $^{c}1400$ |

NOTE.–$z$ is the redshift, and $P$ is the precession period measured in the observer's reference frame $P=(1+z)\,P_{prec}$.
REFERENCE.–a. Caproni et al. 2004; b. Wang & Zhang 2003; c. Rokaki et al. 2003; d. Decarli et al. 2011.